

# **FINAL TECHNICAL REPORT**

## **HRL CONTRACT RFP No. 9060-2**

### **DARPA Physical Intelligence Project - Research Thrust**

#### **“Intentional Action-Perception through Random Graph Theory”**

Submitted to: Dr. Narayan Srinivasa, Manager, CNES, HRL, Malibu, CA  
Prepared by: Dr. Robert Kozma, PI, First Tennessee University Professor  
Department of Mathematical Sciences, University of Memphis, TN  
Period: October 1, 2011 – December 20, 2013  
Date: December 12, 2013

---

#### **Project Objective**

The objective of the University of Memphis (UoM) team has been to utilize neuropercolation theory of the neuropil as a constructive method for developing a novel model of the intentional action-perception cycle as a manifestation of the Physical Intelligence principle.

This work uses Walter Freeman’s neuroscience insights manifested in his hierarchical brain model. The theory is studied using a thermodynamics-based random cellular automata model. The proposed approach interprets intelligent behavior as a sequence of intermittent spatial patterns, each of which provides a prediction of the future action to be taken, and which is initiated and terminated by phase transitions in an open system. Each pattern is sustained by a limit cycle attractor with symmetry breaking on close approach to the transition point and restoration by synchronization-desynchronization effects in the spatio-temporal dynamics. The model is expected to demonstrate emergent intelligence when implemented on a suitable platform allowing a goal-oriented intentional system to interact continuously with its environment.

#### **Research Approach**

- This project uses neuroscience insights manifested in Freeman’s hierarchical brain model, the K sets, including K0, KI, KII, and KIII.
- Our approach interprets intelligent behavior as a sequence of intermittent spatial patterns, each of which provides a prediction of the future action to be taken.
- Spatial activity patterns in the cortex are separated by phase transitions between high-dimensional (chaotic) and low-dimensional (liquid-like) dynamic states.
- Phase transitions are described using the neuropercolation model system based on hierarchical random cellular automata that implement Freeman K-sets.

- The developed model is employed to demonstrate emergent intelligence when implemented on a suitable platform allowing a goal-oriented intentional system to interact continuously with its environment.

## Team

The UoM team includes:

- Prof. Robert Kozma (PI), Prof. Paul Balister, and Prof. Bela Bollobas (also affiliated with Cambridge University, UK),
- Prof. Marko Puljic (Tulane U) and Prof. Walter J Freeman (UC Berkeley) who act as consultants to this project.

## Achievement Statement

The research has been conducted according to the SOW in the following tasks:

Task 1.1. Theory and modeling of intentional action-perception cycles using hierarchical dynamic models (until 5/2012).

Task 2.1. Basic models of structural evolution and learning in geometric random graphs (until 5/2012).  
Continued through tasks 1.6.1 and 1.6.2 (11/2012-12/2013).

Task 3.1. Develop tools for computational analysis of intentional dynamics (until 5/2012).

The planned goals have been accomplished in all task areas.

## Major achievements

1.1.A Provided theoretical justification and detailed technical description for the four components of the generalized Carnot cycle in brains operating far from equilibrium, whereas metabolic energy is converted into meaningful action and knowledge as an open thermodynamic system.

1.1.B Constructed hierarchical brain models following Freeman's 10 basic principles of neurodynamics. During the present project, we established the first five building blocks of neurodynamics using neuropercolation model system.

2.1.A Established mathematical models for rigorous formulation of metastable, self-organized critical dynamics on n-dimensional tori and conjectures about the onset of phase transition dynamics in such models.

2.1.B Quantitatively characterized the evolution of the neuropercolation network parameters as the function of rewiring in 2-dimensional KI lattices.

1.6.1A The conditions of the onset of critical states with large-scale synchronization of a narrow-band carrier wave have been established in KII and KIII sets. This result is crucial for the

description of the system's response to known stimuli, thus providing a robust and very rapid recognition and recall of previously learnt input patterns.

- 1.6.1B Large-scale computer simulation methods have been conducted to describe structural features of lattice graphs. Provided quantifiable statistical characterization of heterogeneous random graphs and the generation of cell assemblies. Determined graph-theoretical features such as mean path length and cliqueness.
- 1.6.1C In response to the feedback from DARPA project management, we intensified the collaboration with other teams in the PI project. Worked with UCLA team on hardware implementation of the neuropercolation model system on complex atomic switch array (CASA) platform.
- 1.6.1D Employed KI level neuropercolation to interpret the dynamical behavior CASA array with of Ag filaments, including the formation of metastable activity patterns due to phase transitions at the Ag/Ag<sub>2</sub>S/Ag interface. Our studies indicate that input voltage level may serve as a control parameter to drive the system toward sustained, self-organized critical states.
- 1.6.1E Joint work has been conducted with SRI team members on evaluating scale-free behavior of power spectra obtained for learning the T-maze problem.
- 1.6.1F Statistical properties of the neuropercolation model has been studied and linked to recent developments in extreme and super-extreme catastrophes. Phase transitions in neuropercolation models can be interpreted as Dragon Kings (DK), which go beyond standard self-organized critical models.
- 1.6.1F Neuropercolation approach has been used for the description of spatio-temporal dynamics in brains, including "Rich Club" (RC) structures, which we describe as "Pioneer Neurons." Competitive advantages of neuropercolation approach have been documented in a comprehensive description of brain dynamics.
- 1.6.2A Neuropercolation models with various topological structures have been studied near the critical state. Reinforcement learning with Hebbian correlational learning rule and also habituation has been studied.
- 1.6.2B Learning effects have been studied in coupled oscillatory layers, modeling action-perception dynamics. Without learning and in the absence of input patterns, broad-band (chaotic) oscillations are observed at the control output. Following learning, specific inputs generate narrow band oscillations indicating that the system recognized the learned stimulus.
- 1.6.2C Successful learning has been demonstrated in neuropercolation model using various input patterns. The trained system showed robust recognition performance for classification problems under various operating conditions.

1.6.2D Documented drastic improvement in the clustering performance of data-processing algorithms when using Hebbian learning in KIII-based cognitive filters as data preprocessing devices.

3.1.A A novel model for the cognitive cycle has been described based on the re-analysis of intracranial ECoG data from Freeman Neurophysiological Lab. We introduced well-defined steps in the cognitive cycle and identified relevant statistical measures for their quantitative characterization.

3.1.B The following steps are defined for the characterization of the cognitive process: (i) initial registration of the sensory stimuli ('awe' moment); (ii) chaotic exploration of the memory landscape; (iii) recognition of the stimuli and decision making ('aha' moment); (iv) integration of the new knowledge into the memory landscape; (v) and return to background activity of alertness.

## Task 1.1 Theory of Intentional Perception-Action as a Carnot Cycle (until 5/2012)

### Task Outline

Establish the theory of the generalized Carnot cycle as the result of the unique properties of the neuropil medium, by defining and plotting the four isoclines suggested by Dr. Freeman's far-from-equilibrium thermodynamic model. In the model, the conventional coordinates of energy and entropy are replaced by the time-dependent coordinates of the rate of change in entropy and the rate of energy dissipation (power), and rate of loss of free energy.

### Research Approach

We model the Action-Perception-Assimilation (APA) cycle as an open thermodynamic system operating in interaction with the environment. Each APA cycle commences by a phase transition, in which the immense population comprising each sensory cortex condenses from a gas-like state to a liquid-like state. It concludes with return of the cortex to the expectant gas-like state. Carnot used his diagram to estimate the work done in each cycle. We model the macroscopic thermodynamics with the generalized Carnot cycle, in which the energy required for the construction of knowledge is supplied by brain metabolism and is dissipated as heat by the cerebral circulation.

A basic quantity analyzed is neurophysiological experiments is PSD(f) - power spectral density function in frequency f determined using Fourier transform. We distinguish between temporal frequency in Hz, PSDt(f), and spatial frequency in cycle/mm, PSDx(k). This distinction is especially important in the spatial analysis of high density ECoG and EEG.

In addition to PSD, we use the analytic power as a measure of the rate of energy dissipation in the subcritical, critical, and supercritical domains. Hilbert transform-based analytic signals are useful in the case of nonstationary, non-Gaussian processes, as the ones observed in brains. The instantaneous phase is a suitable measure to quantify transitions between synchronous and nonsynchronous regimes. Such analysis allows direct comparison with experimental data on brain dynamics.

### Project Results

Experimental evidence is presented that the Carnot cycle with isothermal processes, coupled by adiabatic cooling and heating, can be used to interpret the cognitive process. We postulate that the action-perception-assimilation cycle comprises a sequence of consecutive Carnot cycles required for perception, assimilation, and action, depending on the complexity of the cognitive task at hand.

We subdivide the cognitive process in each burst into four stages. We used the area to index the amount of knowledge created by each burst, see Fig. 1.

1. In stage 1-2 (binding and coherence): Conditioned stimulus carried by a microscopic volley of action potentials from receptors ignites a mesoscopic Hebbian assembly that generalizes input to a category of equivalent receptors, abstracts by removing irrelevant

detail, amplifies the volley, and selects a basin of attraction in cortical memory. The binding in the assembly and the convergence to an attractor decrease the disorder and entropy.

2. In stage 2-3 (condensation and transmission): The ignition of the Hebbian assembly provides mesoscopic transition energy that initiates a macroscopic, spatially coherent burst of oscillatory dendritic current that carries the spatial AM pattern. The low-density chaotic activity governed by a point attractor and synaptic transmission undergoes a phase transition by condensing to a high-density narrow-band activity that is governed by a limit cycle attractor, shaped by synaptic transmission, and empowered by ephaptic transmission. Masses of neurons are recruited in coherent subthreshold oscillations, so that all neurons in the coherent domain can contribute their bits of information to the recalled knowledge. The burst is not a representation of a stimulus; it is a complete memory of the stimulus. The macroscopic pulse cloud shaping and shaped by the dendritic current field down-samples the AM pattern, using time multiplexing and pulse density modulation in cortical columns.
3. In stage 3-4 (uncoupling and decoherence): The cortex transmits the burst through a fan-out-fan-in tract that performs a Gabor transform, which amplifies the coherent carrier, attenuates all else as noise, and delocalizes the perceptual content. In this form the AM patterns from all modalities can be integrated by linear matrix concatenation. Frequency dispersion enhances disorder by interference due to phase dispersion.
4. In stage 4-1 (evaporation): Declining power due to recovery processes manifested in refractory periods evaporates the signal after a duration that is proportional to the width of the pass band. Extremely low values of analytic power appear at spatiotemporal points in cinematic displays of the ECoG, indicating the presence of a singularity in cortical dynamics that mediates the phase transition of neuropil from the liquid-like phase governed by a limit cycle attractor to the gas-like phase governed by a point attractor.

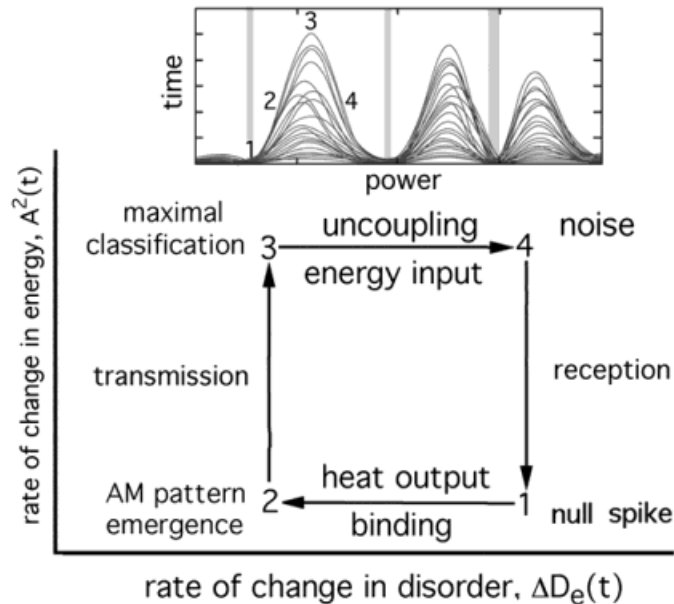


*Figure 1. Illustration of the generalized Carnot cycle in the neuropil medium. The coordinates are expressed in terms of two variables that can be measured using the ECoG. The squared analytic amplitude measures the rate of energy change in the cortical tissue, while the distance between consecutive amplitude modulated (AM) patterns measures the rate of change in the disorder.*

## **Task 2.1 Mathematical modeling of the evolution and learning in geometric random graphs and cellular automata (continued as Task 1.6.1 from 11/2012)**

### **Task outline**

Study geometric random graphs, the structure of which evolves in time. Start with modeling single-layer networks corresponding to KI model. Implement various adaptation approaches to modify the system behavior. Consider several evolution/learning rules at various time scales, including the exponentially growing graph with scale-free properties, preferential attachment rule, majority voting, as well as correlation learning rule (Hebbian), reinforcement, homeostatic regulation, and others. Deliverables include mathematical description of the expected behavior of evolving networks with select learning rules.

### **Research Approach using Neuropercolation Model System**

Neuropercolation models are based on powerful tools of random graph theory to develop rigorous models of brain networks. Neuropercolation incorporates cellular automata and percolation theory in random graphs that are structured in accordance with cortical architectures. Random graphs and percolation theory provide a suitable mathematical approach to describe phase transitions and critical phenomena in large-scale networks.

Neuropercolation is a natural mathematical domain for modeling collective properties of networks, especially near critical states, when the behavior of the system changes abruptly with the variation of some control parameters. Critical parameters of neuropercolation include noise (thermodynamic temperature), proportion of nonlocal connections (long axons), and proportion of inhibitory units (negative feedback). In the analysis we rely on Binder's finite-size scaling theory, which has been used successfully to describe critical phenomena in statistical physics domain.

Neuropercolation implements a hierarchy of cellular automata starting from single-layer 2D lattices, to multi-layer models. The network hierarchy and corresponding dynamics implement Freeman's dynamic approach to brain operation and cognitive functions, specifically the 10 building blocks of neurodynamics. Building blocks 1-3 describe the emergence of non-zero background activity and narrow-band oscillations in coupled systems with negative feedback. Chaotic dynamics and intermittent large-scale synchronization are produced by two or more coupled oscillators. If the connected oscillators with different frequencies cannot agree on a common mode, yet cannot ignore each other, together they may generate broad-band chaotic activity. In these systems, we identified four critical points which demarcate various dynamical regimes, including chaos, and large-scale narrow-band synchronization states.

The above results have been used to interpret emergent synchrony in the cortical tissue. We hypothesized that the aperiodic background state with is the manifestation of Freeman's fourth building block of neurodynamics and leads to the formation of metastable activity patterns. At the same time, the large-scale synchrony with narrow-band bimodal, periodic oscillations can be the indication of transitory regime initiated by the positive identification of a stimulus.

## Project Results

1. We modeled two basic operational modes of cortex.
  - One mode describes quasi-stable amplitude modulation (AM) patterns, while the other mode describes rapid transitions from a given AM pattern to another. We model transitions in the 2D lattice representing the cortical layer as bootstrap percolation.
  - We postulate that such percolation process is supported by a Hebbian neural assembly selected by and corresponding to the given sensory input under the specific internal dynamic state of the cortex. The quasi-stable AM oscillations may be modeled by avalanche dynamics, manifesting self-organized criticality (SOC).
  - These two basic operational modes interface through a critical transition point defined by the onset of super-threshold oscillations. We hypothesize that the cumulative curvature measure of clusters may act as an order parameter according to Haken slaving principle. The curvature exceeding a critical value may enforce critical transitions as the function of the random background noise level.
2. We studied properties of our exponentially expanding brain graph model (EEGm). The concept we introduced on “Pioneer Neurons” (PN) sub-plates can be used for describing developmental data on brains. Similar effects have been described as rich “Rich Club” (RC) features. RC is a network property that happens when the hubs of a network, the nodes with largest number of neighbors, are densely interconnected. We show that our EEGm model is characterized by RC property due to the key role of pioneering neurons. In addition to RC feature, the exponentially exploding brain model (EEGm) reflect important experimentally observed properties of brain networks, including short processing paths, the existence of massive parallel processing paths, and the emergence of hub structures with modular architecture.
3. We studied the rapid propagation of phase gradients in the cortex and their cognitive relevance. We introduced the hypothesis that phase dispersion over the hemisphere is the manifestation of the cognitive broadcast as described in Baars’ Global Workspace Theory (GWT). We demonstrated that intermittent synchronization in the neuropercolation model is in accordance with experimental findings. Our ECoG experimental studies indicate that phase desynchronization and the collapse of analytic amplitudes are associated by the ‘aha’ effect of cognitive processing.
4. Power-law statistics became ubiquitous in analyzing extreme events in nature and society. Neuropercolation model of cognition goes beyond self-organized criticality (SOC) and the corresponding fundamental scale-free behaviors, due to the intermittent phase transitions between gas-like and liquid-like dynamic states. Near critical brain states, we observe intermittent desynchronization over large cortical areas for a short period. This is the period of phase transition (PT), when large phase gradients travel rapidly across the cortex. Such phase transitions are a way to interpret “Dragon King” (DK) effects in natural phenomena.

5. We introduced a link between phase transitions in neuropercolation and the concept of "Dragon Kings." Dragon Kings were suggested to characterize extreme and super-extreme events related to dynamical regimes beyond self-organized criticality (SOC). Neuronal avalanches may belong to both SOC and super SOC categories. Neuropercolation model system can contribute to the understanding of generating mechanisms of Dragon Kings in general and to large activation clustering in neural systems, in particular, by using the conceptual and mathematical framework of neuropercolation. Simulation results showed see Fig. 2, the transition from self-organized critical regime to intermittent super-criticality. Around the critical point we observe super-exponential increase in the size of the neural activation clusters, which may indicate the emergence of dragon kings.

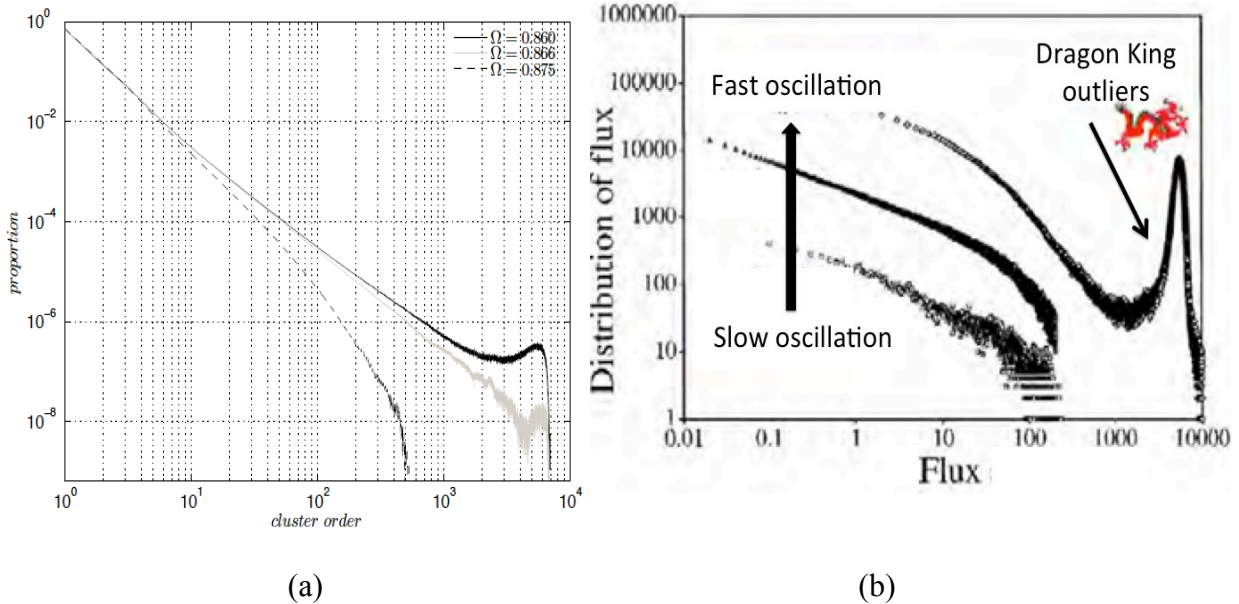


*Figure 2. Illustration of emergence of deviation from scale-free distributions; (a) critical clustering in the neuropercolation model, where omega (describing noise effect) acts as a control parameter; (b) distribution of flux with increasing oscillation frequency; for details, see (Sornette, Quillon, 2012). Increasing deviation from scale-free distribution emerges towards the large tails, as potential manifestations of Dragon Kings (supercritical regimes).*

6. Statistical properties of the evolving graphs have been evaluated, including the mean path length between two nodes, and cliquishness. To measure the cliquishness of a graph, first we select a given node ( $v$ ) and consider its neighbors ( $N(v)$ ). We calculate the proportion of pairs of neighbors of  $v$  that are themselves neighbors ( $C(v)$ ). Finally, we calculate the average of  $C(v)$  as  $v$  runs over all the vertices  $\langle C(v) \rangle$ , which defines the cliquishness value. We studied the mean path length and cliquishness as the function of the rewiring in the case of the KI lattice graph in 2-dimensional lattice. The degree of rewiring is given by  $|R|/|V|$ , where  $|R|$  and  $|V|$  stand for the number of vertices with an edge rewired and the total number of edges, respectively. We conclude:

- The mean path length drastically decreases with a small level of rewiring. The cliquishness, on the other hand, continuously decreases from its max value to 0 as the rewiring increases. These statistical results are important for the learning in the neuropercolation model when Hebbian assemblies are formed, which are expected to have increased clustering and cliquishness, and decreased path length across the system.
- In modeling cortex, clusters/cliques are postulated to form among sites selected by stimulus inputs during learning, leading to the formation of Hebbian nerve cell assemblies in reinforcement learning, in accord with the rule: “neurons that fire together wire together”. These are not small worlds; they are tightly coupled networks that amplify, generalize and abstract over categories of input. We postulate that they also determine the trajectory of cortical dynamics by directing it into the basin of an attractor, so that the cortex generates an appropriate spatial AM pattern of a carrier wave.

7. The effects of rewiring have been studied quantitatively in the neuropercolation model. The basic random graph with regular structure has nearest neighbor connectivity. We conclude:

- In cortex the log density of connections falls with distance exponentially or with log distance linearly. It may approximately conform to log-log, hence supporting scale-free dynamics, which is an important clue for explaining how cortex sustains very long correlation lengths and exceedingly rapid global phase transitions.
- In small world random graphs and in neuropercolation simulations a small proportion of nearest neighbor connection is replaced by long connections selected at random. A proportion of long connections is clearly important in random graphs and equally so in nonlinear cortical dynamics as the basis for rapid phase transitions to relatively enormous domains of coherent oscillation.
- The long connections do not lead to cliques by themselves. That would require breaking of symmetry in the sense of departing from uniformity of spatial density distribution of long connections. Cliquishness and clumping are to be imposed by learning. Clumping implies only local increases in density with sequestration by diminution of connection density. Long-range connectivity permits formation of widespread Hebbian cell assemblies that enhance generalization over widely dispersed sensory inputs.

## **1.6.2 Mathematical modeling of learning in hierarchical geometric random graphs (starting from 11/2012)**

### **Task Outline**

Extend the results obtained in Task 1.6.1 with the evolution of single-layered geometric graphs to higher order, multi-layer networks. If needed, apply empirical methods to achieve quantifiable results. Test the hypotheses about the presence of intermittently propagating phase gradients during learning and recall, which correspond to experimentally observed cognitive activity and decision-making. Deliverables include evaluation of the system behavior with and without learning, quantification of learning effects and description of measurable spatio-temporal correlates of intelligent behavior.

### **Research Approach**

We have conducted massive computational simulations using random cellular automata models. We developed methods to evaluate the system state with respect to criticality by generalizing Binder's criterion using 4<sup>th</sup>-order cumulants based on finite-size scaling theory. The task requires very significant computational efforts, thus computing efficiency is critical. In order to achieve the required statistical accuracy for Binder finite-size scaling theory, we need to calculate 100 points for varying parameter value (noise), and each point is evaluated following at least 20,000,000 iterations. Most of our computations are executed on the UoM massive parallel computing facility, where we use the maximum allowed computational power. In the Spring 2013, we finally had access to DoD HPC facilities. Due to the summer maintenance and the termination of our project, we were not able to benefit from this additional computational opportunity in the present project ending December 2013.

### **Project Results**

#### **Oscillator Created by Interacting Excitatory and Inhibitory Neuropercolation Layers (KII)**

1. Broad-band activity with  $1/f^{\alpha}$  power spectra is observed for unlearnt conditions. On the other hand, Hebbian learning results in the onset of narrow-band oscillations indicating the selection of specific learnt inputs; see Fig. 3. These observations demonstrate the required properties according to Freeman's building blocks of neurodynamics.
2. We determined boundaries of large-scale synchronization domains with narrow-band oscillations; for the illustration of the dynamics of the synchronized state. The large-scale, intermittent, narrow-band synchronization is characteristic of a metastable system at the edge of criticality, when input-induced or spontaneous transitions can destabilize the chaotic basal state and push it to a quasi-limit cycle oscillatory regime. Our results indicate that the introduced Hebbian learning effect can be used to identify and classify inputs, and potentially using it for pole balancing control task.

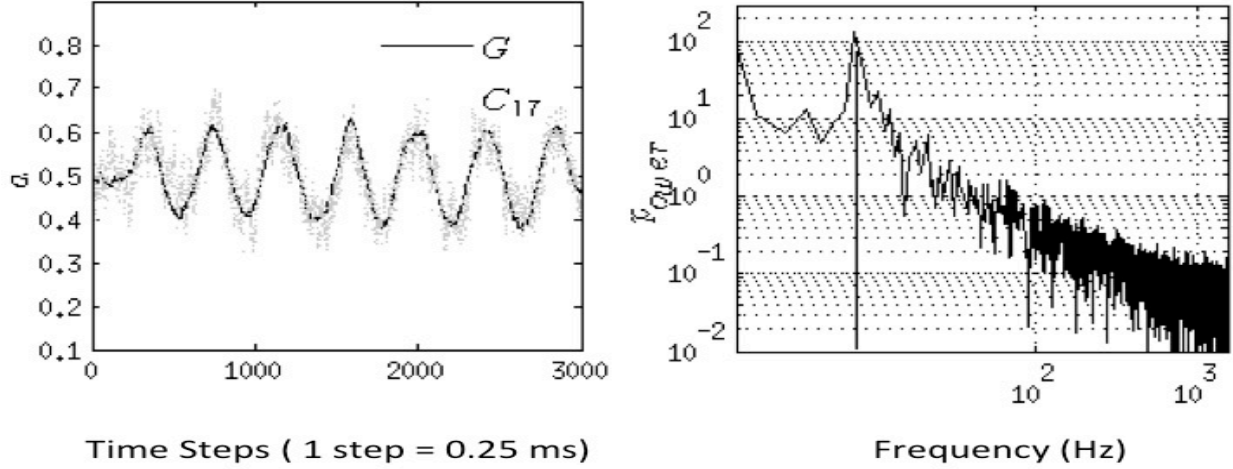


*Figure 3. Illustration of the dynamic state with narrow-band, synchronous oscillations; left plot shows time traces of activity (a) for the ensemble average (solid line), and channel #17 (dash); right plot is the Power spectrum showing a prominent oscillation frequency (approx. 10 Hz in this simulation).*

### Two interacting Oscillators (KIII simple version)

3. We modeled two interacting oscillators, which correspond to different cortical areas. We studied the influence of various parameters on the critical behavior of this coupled system, including noise level, proportion of non-local connections after rewiring some local links, strength of inhibition, and strength of connections between cortical areas. In the KIII model, multiple critical points are found, which demarcate various dynamic regimes, such as unimodal (paramagnetic) state, bimodal large-scale synchronization, multimodal broad-band (chaotic) oscillations, mixed broad- and narrow-band regimes.
4. In the system with two oscillators, there are four critical points  $\omega_0 < \omega_1 < \omega_2 < \omega_3 < \omega_4$ , corresponding to decreasing noise levels ( $\omega=0$  is very high noise and  $\omega=1$  means no noise). When  $\omega < \omega_0$ , aggregate activation distribution is uni-modal (1) and shows paramagnetic regime. When  $\omega_0 < \omega < \omega_1$ , the oscillators exhibit large-scale synchronization and the activation distribution is bi-modal (2). When  $\omega_1 < \omega < \omega_2$ , the two coupled oscillators with different frequencies cannot agree on a common mode, so together they generate aperiodic background activity (chaos). When  $\omega_2 < \omega < \omega_3$ , only one oscillator oscillates in a narrow band and the activation distribution is okta-modal (8). For  $\omega > \omega_3$  neither oscillator oscillates and activation distribution is a hexa-modal (16) describing a ferromagnetic state.
5. These results are illustrated in Fig. 4 using Binder finite-size scaling theory for critical analysis. According the Binder's statistical theory, the intersection point of statistical moments (in our case 4<sup>th</sup> moments) calculated for various system sizes (96x96 and 120x120)

give the critical states with size invariance. In Fig. 4, the various regimes are indicated: paramagnetic (leftmost), large-scale synchrony (white bar), intermittent chaos (black), okta-modal (gray), and ferromagnetic (rightmost) region, respectively.

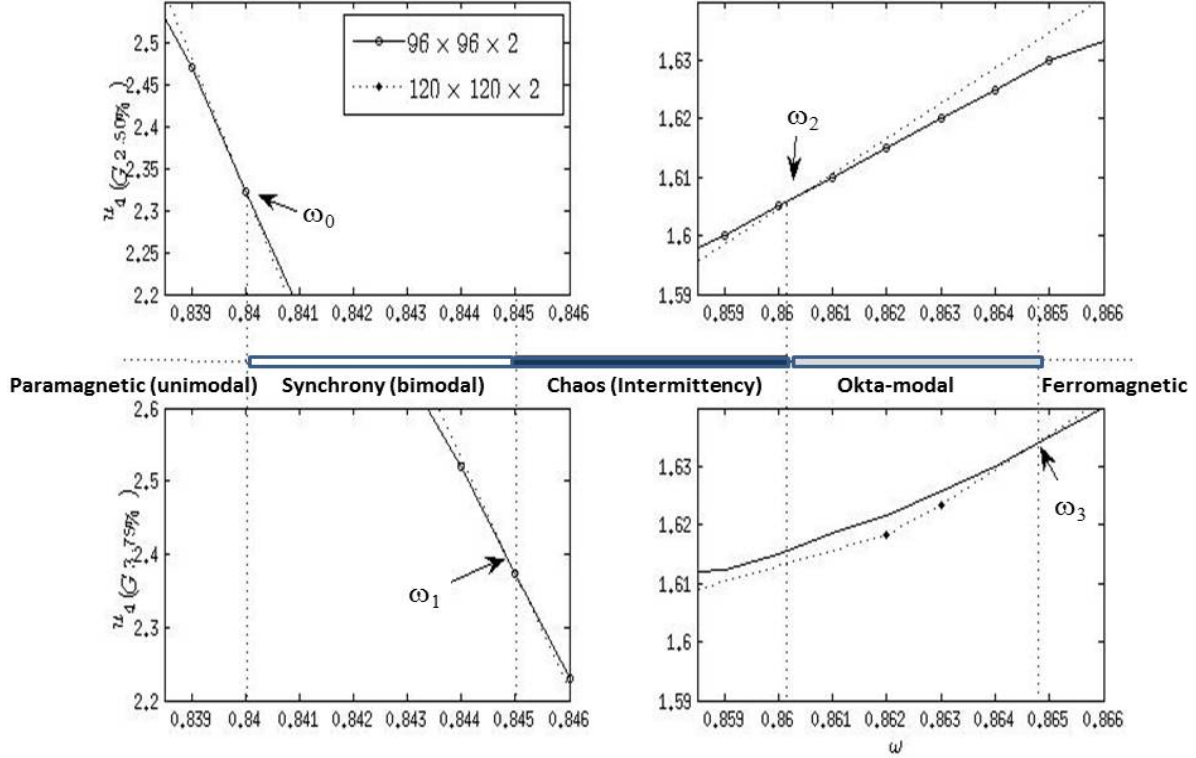


Fig. 4.: Illustration of the identified synchronization regimes for coupled oscillators. Oscillator A is coupled with 2.5% edges (top display), while oscillator B is with 3.75% edges (bottom plot). Five different regimes have been identified from left to right: paramagnetic, synchronous bimodal, chaotic intermittent, okta-modal, and ferromagnetic with hexa-modal distribution functions, respectively. Solid curves indicate coupled lattices of size 96x96, while dotted lines stand for lattice size 120x120.

6. The above results have been used to interpret emergent synchrony in the cortical tissue. We hypothesize that the aperiodic background state with  $\omega_1 < \omega < \omega_2$  is the manifestation of the fourth building block of neurodynamics and leads to the formation of metastable activity patterns. At the same time, the large-scale synchrony with narrow-band bimodal, periodic oscillations can be the indication of transitory regime initiated by the positive identification of a stimulus by a Hebbian assembly.

### Three Interacting Oscillators (Complete KIII)

7. We studied the model of 3 interacting oscillator layers, inspired by the olfactory system. This model uses input (odor) distributed on the input layer and scalar output (classified odor). In

the basal mode without learning, the 3 double layers can generate broad-band chaotic oscillations, see Figs. 5b and 5d; where (d) is zoomed in version of (b). The spikes in Fig. 5a & 5c indicate the presence of input signals. Inputs have been implemented by flipping 5% of the input layer nodes to state ‘1’ (active) for the duration of 20 iteration steps. During the Hebbian correlation learning stage, inputs are introduced 40 times (20 steps each), at regular intervals of 500 iteration steps. Without learning, the activity returns to the low-level chaotic state soon after the input ceases.

8. Figure 6 shows the effect of learning. Learning has been maintained during the 20 step periods when input was introduced. We use Hebbian learning, i.e., the weight from node  $i$  to node  $j$  is incrementally increased if these two nodes have the same state (1-1 or 0-0). The weight from  $i$  to  $j$  incrementally decreases if the two nodes have different activations (0-1 or 1-0). Fig. 6a shows that a narrow-band oscillation becomes prominent during learning, when a specific input is presented. After learning, the oscillatory behavior of the lattice dynamics is more prominent, even without input, but the learnt input elicits much more significant oscillations. This is the manifestation of the 6<sup>th</sup> and 7<sup>th</sup> principles of Freeman’s neurodynamics, and it can be used to implement classification and control tasks.

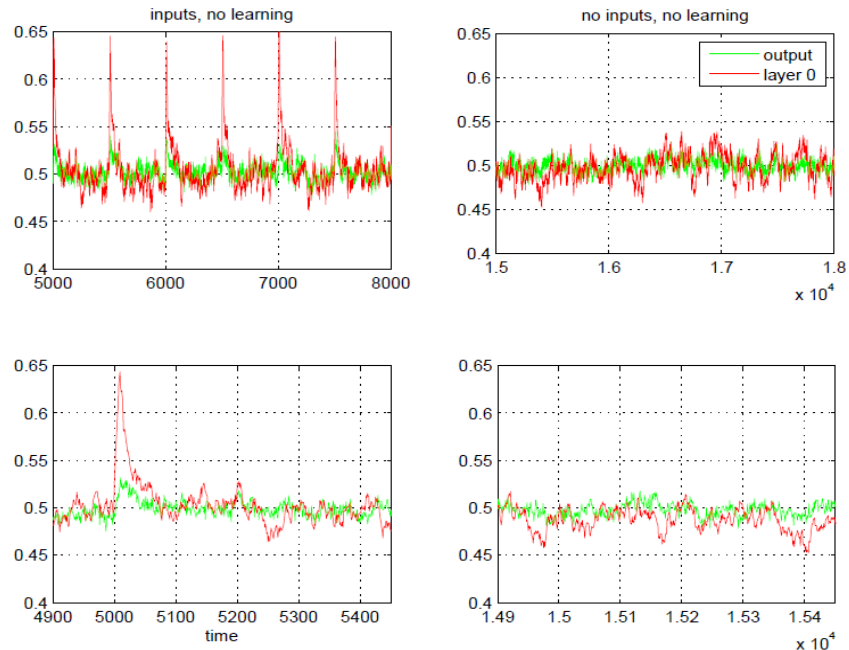


*Figure 5. Activity levels without learning; first row contains (a) and (b) plots, 2<sup>nd</sup> row (c) and (d). Input spike is shown at every 500 steps. The activity returns to base level after the input ceases.*

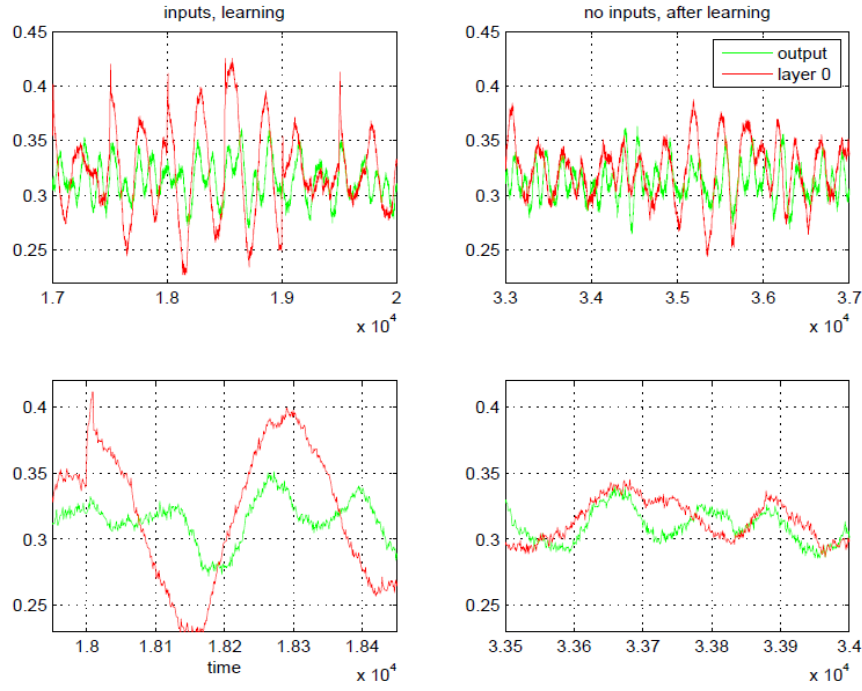


Figure 6. Activity levels with learning; first row contains (a) and (b) plots, 2<sup>nd</sup> row has (c) and (d). Input spike is shown at every 500 steps. The oscillations are prominent during learning and maintained even after the input step is removed (decayed).

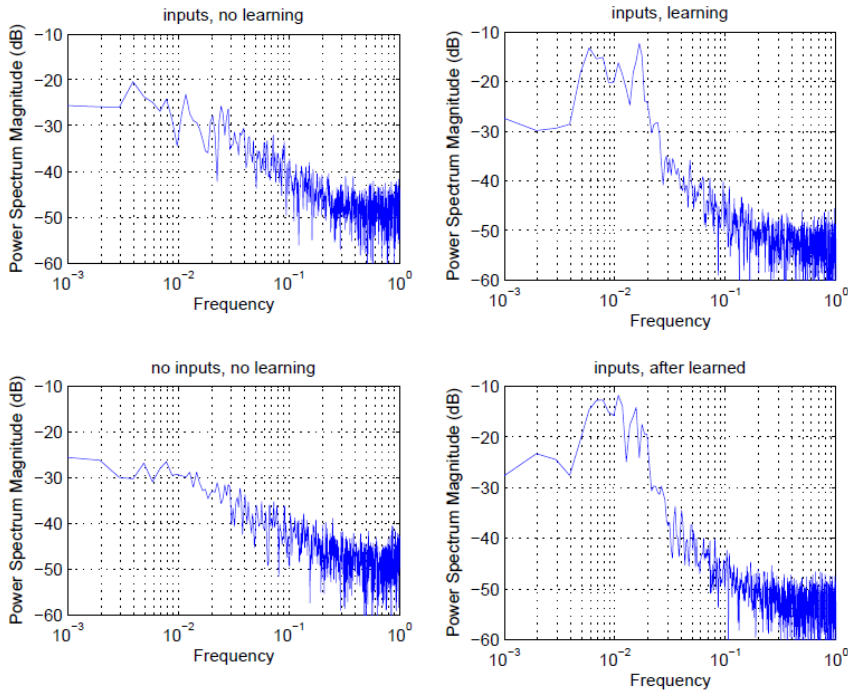


Figure 7. PSD functions without learning (first column) and with learning (second column). Without learning the PSD has scale-free,  $1/f^\alpha$  shape. Prominent narrow-band oscillations are observed as the result of learning. This spectral effect can be used to quantify the learning effect and use it for controlling the balance of the input.

9. We implemented and tested learning algorithms (Hebbian and habituation) in neuropercolation models with various input patterns. Present evaluations are based on average activation level in the output patterns. This is illustrated in Fig. 8, where the time evolution of the average activation ( $a_G$ ) is shown during learning and testing of Input Patterns 0 and 1, respectively. There is a consistent and quantifiable increase in average activity for the learnt pattern 0.

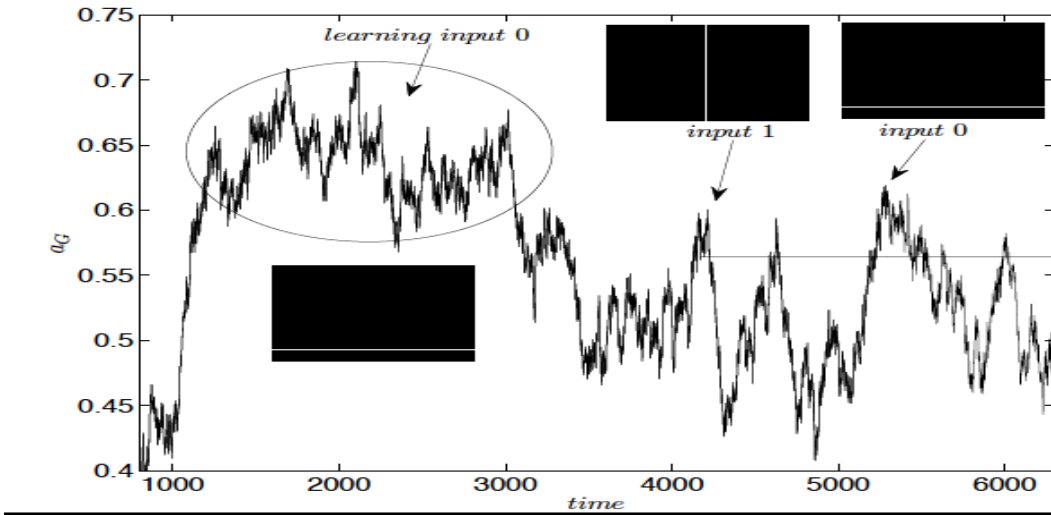


Figure 8. Time evolution of learning and testing input patterns in the neuropercolation model; here  $a_G$  shows the average activity level across the array. The input patterns include stripes of various orientations to demonstrate the classification ability of the trained system.

10. We developed quantitative measures to evaluate the performance of the hierarchical KIII model, and demonstrated significant advantages regarding stability indices of clustering algorithms. We used KIII as a cognitive filter before applying a range of clustering algorithms, including self-organized maps, k-means, hierarchical, model-based and other clustering. The clustering results have been evaluated using a range of validation indices, including stability, external, and internal index measures. The main results are summarized as follows:

- KIII shows very significant improvement (50% improvement or more, in average) in classification performance using stability indices, including average distance between means, figure of merit, average proportion of overlap.
- KIII can be employed as a data filter to transform the input information into an integrated data format, in which the various attributes develop mutual dependence

and demonstrate distributed representation of the inputs in a more robust, distributed format.

- In addition, the first two principal components after KIII filtering contain 82% of data variance in average for the used datasets, which points to the possibility of more efficient encoding of data using KIII processing.

## Neuroporation Model System Implementations on CASA Hardware Platform

### Goal of the Effort

In concert with UCLA/CASA team, efforts have been made to implement neuroporation model on CASA hardware domain. The work focuses on the implementation of basic single-layer, homogeneous (KI) neuroporation model by CASA. Progress has been made in understanding the behavior of the CASA layer by determining characteristic temporal and spatial scales and transfer characteristics based on data readouts from the existing devices by 2x2 and 4x4 electrodes. Data are of courtesy UCLA/CASA Lab, discussions with Jim Gimzewski, Adam Stieg, Henry Sillin, Brian Shieh, Odo Avizienis are appreciated.

### Research Approach

We analyzed the experimental data obtained on CASA Atomic Switch network platform, Bi50-500, over 4x4 arrays. In the experiments, 1V potential was applied at electrode #15 for 20 ms, followed by 80 ms resting period, and this cycle repeated for an extended time period. The complete time series contained active and inactive periods, while the ‘trimmed’ time series included only the 20ms active segments concatenated into a continuous series, i.e., the inactive segments have been trimmed. Current readout is from electrode #7, sampling frequency is 10,000 Hz. Step-by-step incremental current (delta-I) has been analyzed.

### Project Results

1. The results obtained for the probability distribution function histograms are given in Fig. 9.

- There is a scale-free general behavior over the range of  $10^{-3}$  to  $10^{-1}$  delta-I values. At low delta-I values (below  $\sim 0.002$ ), the slope decreases and there is a significant deviation between trimmed and untrimmed cases. The trimmed-out segments describe the background noise at basal state (without feeding Voltage), which is concentrated at small delta-I increments. This result also seems justifying the threshold of 0.002 used in CASA files to determine the transition to metastable states.
- The red histogram (full signal) has prominent peaks at delta-I  $\sim 0.2-0.4$ , while the blue (trimmed curve) has a peak at  $\sim 0.1-0.2$ . There is an additional peak in the red histogram at 0.07-0.09. The red peak at 0.2-0.4 is due to the jumps between the 20ms active and 80 ms inactive periods. This peak is eliminated in the blue curve by trimming the basal state time segments. The blue peak at 0.1-0.2 is added in the trimmed curves by gluing together the 20ms segments, which do not exactly match at start/begin.

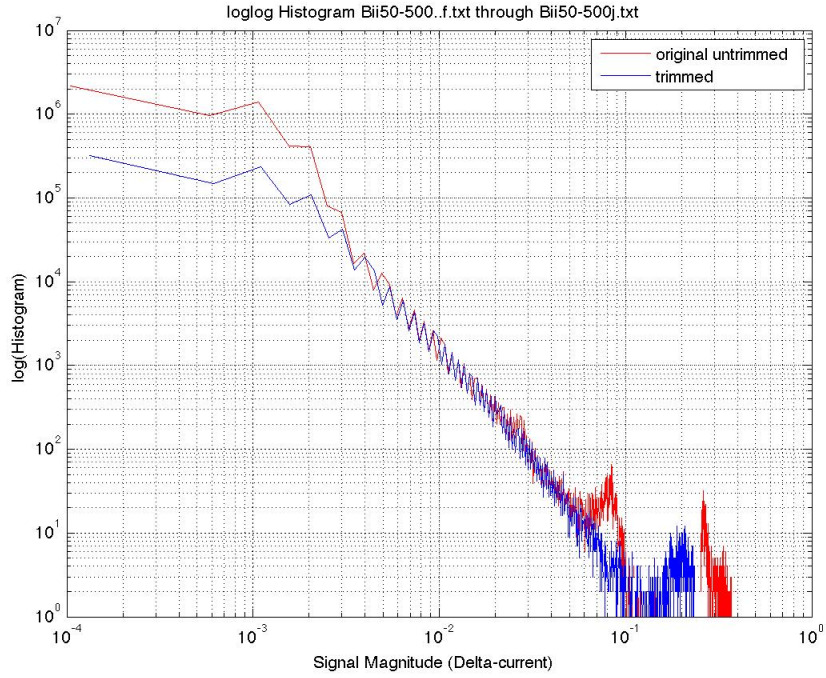


Figure 9. Histogram of the Bi50-500 4x4 array current measured on channel #7. The histogram is determined for the delta current step-by-step change. Red curve shows the total time series, blue curve is the concatenation of the active (20ms) periods, by trimming the 80ms resting periods.

2. We performed statistical analysis of the distribution of the metastable current state levels. Results are as follows: The histogram of the levels of metastable states shows two prominent peaks, at 12-13 uA and 22-28 uA, respectively. There are some less prominent peaks at 30-32 uA and 40-44 uA. There is a broad tail of the histogram until about 100 uA. The two main peaks show the existence of the metastable states. It may be the superposition of several Gaussians, or overlaying Poisson distributions. The width of the peaks is about 5 uA, which is much larger than the thermal background noise. Thus the multi-modal distributions are essential features of the dynamics, much above the background level.
3. We conducted neuropercolation simulations to model the growth of the connectivity in the CASA system with constant or periodic input perturbations. In these models, the noise level is maintained constant while the connectivity increases, to simulate CASA connectivity growth (increasing neighborhood size). Phase transition is clearly identified at neighborhood size of  $\sim$ 16-18 from low magnetization to high magnetization regimes. Phase transitions between highly-organized (ferromagnetic, liquid-like) and less organized (paramagnetic, gaseous-like) states in neuropercolation seem to be feasible interpretations of the transition between “soft” and “hard” switches in ULCA’s ASN; see (Avizienis et al, 2012) for details. Neuropercolation shows how input induces switch in the dynamics, as the operational regime has been adjusted to be near the percolation transition threshold, thus a small input perturbation (produced by learnt stimulus) creates a transition. At the same time no transition

occurs for a perturbation of similar (weak) magnitude, which was not learnt. It is therefore suggested to operate ASN at the boundary between ‘hard’ and ‘soft’ switch regimes.

4. We analyzed CASA experiments with single-channel recording at various current levels. Examples of amplitude distributions are shown in Fig. 10 for various current levels. The distributions approximate a scale-free behavior except for small voltage values (0.4 V).

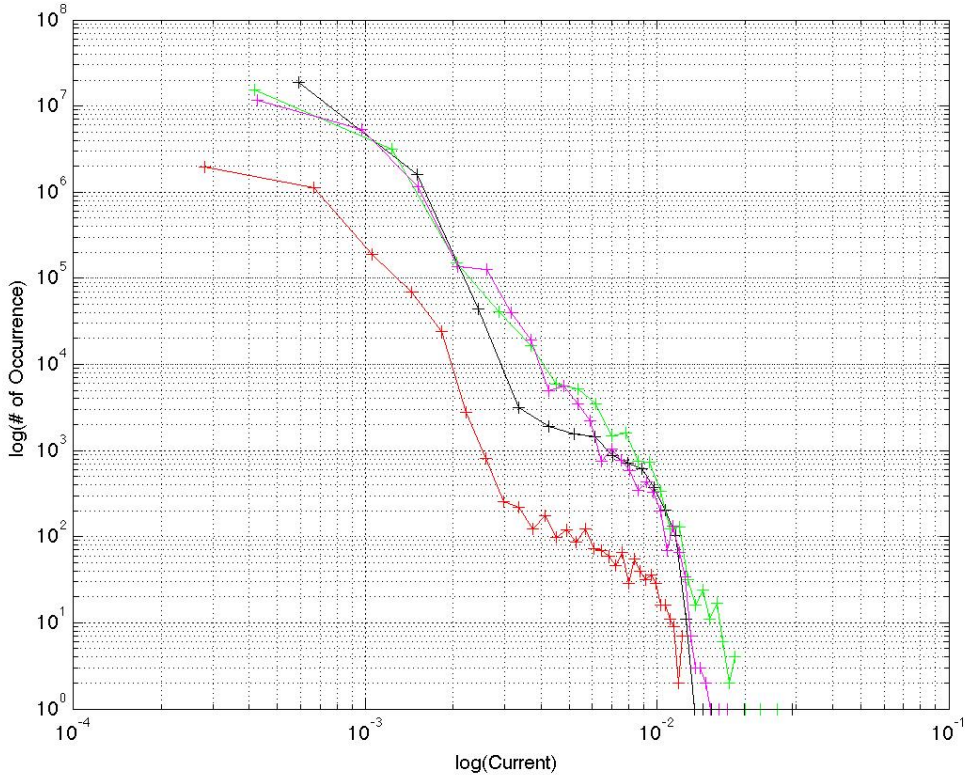


Figure 10. The normalized frequency of occurrence is shown on the vertical axis, during CASA single-channel experiments; the driving voltage levels: red – 0.4V, black – 2.75V, green – 6V, magenta – 7V.

### Discussion on the relationship between neuropercolation and CASA/ASN platform

- **Network structure:** CASA is remarkably appropriate for modeling the topology of cortex as a 2-D planar array of neuropil as distinct from a neural network. Neuropil consists in an exceedingly dense fabric of randomly oriented fibers in the plane having a power-law distribution of connection density with connection distance. The cell bodies are essential for neuropil formation, just as are the copper posts in CASA formation, but along with glia play only secondary supportive roles in system dynamics. The module for modeling state variables is not the neuron but the local matrix of connections. CASA has the option of high density of posts and comparably high density of available contacts among fibers.

- **Readout:** The output of the neuropil is spatially coarse-grained and down-sampled by deep pyramidal cells that perform local spatiotemporal integration over the matrix of superficial pyramidal cells. CASA simulates this neural operation by sampling electrodes placed at spatial intervals in an array near the center of the CASA chip. We have not yet set up a protocol for evaluated the spacing, number and especially the diameters of sampling electrodes needed to perform optimally the spatiotemporal integration required for readout.
- **Contact barriers, synapses:** The sulphurization giving the  $\text{Ag}_2\text{S}$  creates a variable resistor metal-insulator-metal junction (MIM) that is comparable to the relations among neural axons and dendrites in neuropil. Interactions are therefore more likely to be characterized as ephaptic rather than synaptic. The read-out by each sampling electrode appears to be comparable to the operation of local populations of  $\sim 10^4$  deep pyramidal cells that time-multiplex their action potentials, giving a pulse density for output that is suitable for transmission to simulated synapses in read-out neural networks. Some assay is needed of the density of MIM connections with respect to the diameter and spacing of the sampling electrodes.
- **Bistability:** The MIM at the microscopic level has two states: a low conductance state with a crystalline structure characterized as acanthite between Ag surfaces and a high conductance state by a factor  $\sim 10^6$  characterized as argentite. At the macroscopic level of observation the two states are characterized as phases. The phase transitions have the memristive property of pinched hysteresis. The phase transition is in two steps. First, under the application of a voltage difference across the MIM, the Ag aligns into filaments, one of which will form a metallic link across the gap. The resulting jump in current triggers the phase transition from the insulating clumped  $\text{Ag}_2\text{S}$  to a body-centered cubic matrix that gives the macroscopic current surge. This phase transition matches well with the phase transition in cortex in two stages. First is the activation of a Hebbian assembly by a learned conditioned stimulus, which ignites the vigorous firing of a dedicated mesoscopic network that provides the transition energy required for a macroscopic transition of the cortical neuropil from a low-density gas-like phase to a high-density liquid-like phase in perception.
- **KIe Implementation and Background Activity:** The discovery of the possible correspondence between phase transitions between bistable states in KIe and CASA may prove to be of major importance in guiding the work of implementing the KIe set on CASA. The KIe set and CASA both have the property of silence (the 'open loop' state) at rest and oscillatory activity under dc excitatory bias. However, when the connectivity is sufficiently dense the KIe set gives self-sustained, self-regulated background activity that is essential for criticality and the capacity for phase transition. CASA at present lacks the capacity for self-sustained intrinsic background activity. This capacity may be inherent in the high range of the V-I function that UCLA now proposes to explore, in search of factors that intrinsically limit the dynamic range of function short of irreversible damage to CASA. Exploration of the upper range will require refinement in the test input in perturbation. The optimum test input for brain research is the impulse (the Dirac delta function). It is essential for evaluation of the temporal and spatial scaling of the CASA for modeling in terms use for modeling K-sets.
- **Thermodynamic properties:** The UCLA group has displayed a map of the spatial temperature

variations of the chip during maintenance of a metastable pattern of activity. This measure may open a valuable path to modeling the phase transition using the temperature-dependent Ginzburg-Landau equation. This experimental approach is expensive for the requisite imaging equipment, so it would have to be justified first by detailed mapping of the spatial patterns of the analytic power of active states, followed by a theoretical prediction of the spatial patterns of temperature to be sought.

– Conclusions on CASA/ASN and neuropercolation

- The chief asset of CASA is its capacity to simulate the property of ephaptic transmission in cortical neuropil, by which a high energy density is achieved that incorporates the entire chip into transiently coherent oscillation that carries an image with high information content, a complex associative retrieved memory.
- Clumping and clustering may occur intrinsically and at random in ASN, so we may have to deal with it, either stationary or time varying, or both. The mean path length and clustering coefficient are likely to become useful when we have achieved spatial analysis and learning capability, so we should define these properties of random graphs at present in respect to dealing with spatial irregularities inherent in the ASN.
- Learning will require methods for selectively increasing, decreasing or deleting point connections that impose clustering onto the random ASN. Modifiable connections and a mechanism corresponding to reinforcement learning in ASN will be the basis for memory storage. In K-sets the modifiable connections are only among the excitatory cells, so that NP for the KIE-set may profitably be applied to ASN as models cortical dynamics.

### **Collaboration with the SRI team in PI**

Metastable cognitive states can be approximated as self-organized criticality (SOC), with possible transitions between various memory-states. Machine learning tools provided by SRI team are very useful to characterize these states and provide a meaningful readout for external use, e.g., classification, and control. At the same time, neuropercolation can provide the initial conditions for the various metastable states to be processed by reservoir computing tools.

We worked on evaluating the scale-free features of the power spectral density functions obtained by reservoir computing (RC) simulations during the T maze learning problem. Based on statistical considerations, we modified parameters of the evaluation algorithm. As a result, scale-free behavior is observed with changing slope across a range of coupling parameter  $b$ . Figure 11 illustrates power spectra as the function of  $b$ , demonstrating spectra with varying slopes as  $b$  changes.

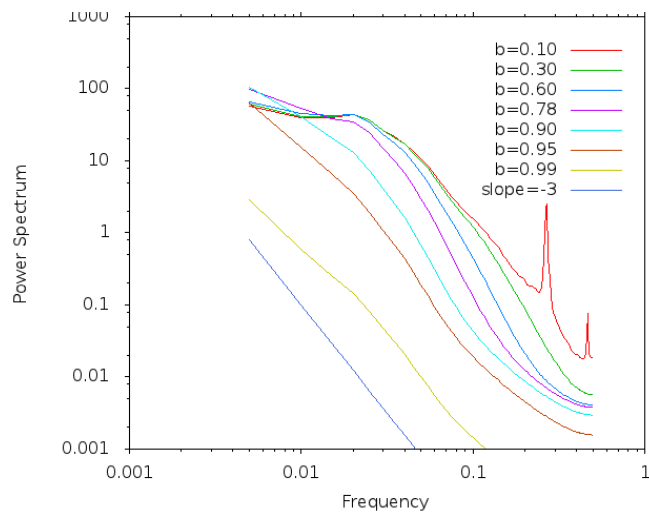


Figure 11: Power Spectra calculated by reservoir computing model during the T maze navigation experiments;  $b$  is the couple parameter (figure is the result of joint work with J Wang and R Rohwer, SRI).

## **Task 3.1. Develop tools for the analysis of the spatio-temporal dynamics (until 5/2012)**

### **Task outline**

Analysis of 2D Random Cellular Automata at various critical conditions corresponds to Freeman's 10 building blocks of neurodynamics. Blocks 1-3 have been implemented earlier. This task focuses on block #4 showing chaotic oscillations and intermittent large-scale synchronization. Study clustering and synchronization measures in a wide range of operating conditions in coupled oscillators.

### **Research Approach**

Spatio-temporal neurodynamics in brains is modeled by Freeman K sets, which form a hierarchy for cell assemblies with the following elements:

- KO sets represent non-interactive collections of neurons with globally common inputs and outputs: excitatory in KOe sets and inhibitory in KOi sets. The KO set is the module for K-sets.
- KI sets are made of a pair of interacting KO sets, both either excitatory or inhibitory in positive feedback. The interaction of KOe sets gives excitatory bias; that of KOi sets sharpens input signals.
- KII sets are made of a KIe set interacting with a KIi set in negative feedback giving oscillations in the gamma and high beta range (20-80 Hz). Examples include the olfactory bulb and the prepyriform cortex.
- KIII sets made up of multiple interacting KII sets. Examples include the olfactory system and the hippocampal system. These systems can learn representations and do match-mismatch processing exponentially fast by exploiting chaos.
- KIV sets made up of interacting KIII sets are used to model navigation by the limbic system.
- KV sets are proposed to model the scale-free dynamics of neocortex operating on and above KIV sets in mammalian cognition.

In this project task, Freeman sets of hierarchy levels KO-KIII are applied for the analysis of ECoG experiments in animals and humans.

### **Project Results**

1. According to our model, sensory stimuli are manifested in the neocortex through the creation of the knowledge necessary for intentional behavior and decision making. These results are interpreted through the concept of pragmatic information, which is complementary to the Shannon entropy Index.
2. We identified large-scale synchronization across broad frequency bands, indicating the construction of knowledge and meaning from input sensory data and leading to awareness

experience. Below are the steps of the cognitive process (with times given with respect to the post-stimulus period):

- Step 1 (0 – 0.1 s):  
Initial impression in response to sensory stimuli, which is termed the “*Awe*” moment. This stage is characterized by high synchronization and low amplitudes across distributed cortical regions.
- Step 2 (0.1 – 0.3 s):  
Chaotic Exploration of memory traces with highly distributed and desynchronized patterns. The amplitude patterns drop dramatically in some regions, also called as “null spike.”
- Step 3 (0.3-0.45 s):  
Recognition/identification of the searched clue/decision and it can be termed the “*Aha*” moment. During “*aha*” moments there is a tendency towards synchronization and the emergence of metastable amplitude patterns.
- Step 4 (0.45 – 0.6 s):  
Next is the stage of integration of the new knowledge in a chaotic dynamic process. Chaotic integration is characterized by strong and widespread “null spikes” as well as the consistent rise in amplitudes.
- Step 5 (0.6 – 0.9 s):  
Finally there is a dramatic drop in the indices toward the end of the post-stimulus brain activity, showing a return to the usual, background level.

## Publication Outcomes of the Project (2011-2013)

### Books (2)

1. Freeman, W.J., R. Qian Quiroga "Imaging Brain Function with EEG - Advanced Temporal and Spatial Analysis of Electroencephalographic Signals" Springer. ISBN 978-1-4614-4984-3. <http://www.springer.com/biomed/neuroscience/book/978-1-4614-4983-6>. (2013)
2. Kozma, R., R. Pino, G. Pazienza (Eds) "Advances in Neuromorphic Memristor Science and Applications," Springer Verlag, Heidelberg, Germany (2012).

### Book Chapters (5)

3. Kozma, R., M. Puljic, W.J. Freeman "Thermodynamic Model of Criticality in the Cortex based on EEG/ECoG data," Chapter in "Criticality in Neural Systems," D. Plenz (Ed.), John Wiley & Sons, 2013 <http://arxiv.org/abs/1206.1108> (in press).
4. Kozma, R., R. Pino, G. Pazienza "Are Memristors the Future of AI? – Review of Recent Progress and Future Perspectives," in "Advances in Neuromorphic Memristor Science and Applications," by R. Kozma, R. Pino, G. Pazienza (Eds) Springer Verlag, Heidelberg, Germany (2012).
5. Kozma, R., "Synchrony, Oscillations, and Chaos in Neural Networks," in: "Handbook of Computational Intelligence – Neural Networks," C. Alippi (Ed.), Springer, 2013 (in press).
6. Kozma, R. "Neuropercolation," in *Encyclopedia of Computational Neuroscience*, R. Jung and D. Jaeger (Eds.), Springer Verlag, 2013 (in press).
7. Kozma, R. "Neural Mass Action," in *Encyclopedia of Computational Neuroscience*, R. Jung and D. Jaeger (Eds.), Springer Verlag, 2013 (in press).

### Journal Articles (8)

8. Kozma, R., Puljic, M. (2013) "Hierarchical Random Cellular Neural Networks for System-Level Brain-Like Signal Processing," *Neural Networks*, 45, pp. 201-110, 2013.
9. Kozma, R., M. Puljic (2013) "Learning effects in neural oscillators," *Cognitive Computation*, Vol. 5(2), pp. 164-169, 2013.
10. Capolupo, A., Freeman, W.J., Vitiello, G. (2013) "Dissipation of 'dark energy' by cortex in knowledge retrieval," *Physics of Life Reviews*, January 2013, on-line. DOI: 10.1016/j.plrev.2013.01.001, <http://authors.elsevier.com/sd/article/S1571064513000134>.
11. Kozma, R. "Mathematical Theories of Physical Intelligence - A Comment," *Physics of Life Reviews* (2013).
12. Kozma, R., J.J.J. Davis, W.J. Freeman (2012) "Synchronization of De-Synchronization Events Demonstrate Large-Scale Cortical Singularities As Hallmarks of Higher Cognitive Activity," *J. Neuroscience and Neuro-Engineering JNSNE*, 1(1), 13-23, 2012.
13. Kozma, R., W.J. Freeman "Cognition as a Neural Percolation Process through the Cortex by Cinematic Phase Transitions," submission to *Behavioral & Brain Sciences BBS* (submitted).
14. J. Rosa, R. Kozma, D. Plazentin, "Freeman KIII Models as Cognitive Filters for

Improved Clustering Algorithms,” *IEEE Trans. Neural Networks and Learning Systems* (submitted).

15. Kozma, R., Puljic, M. “Emergent synchronization and intermittent desynchronization in coupled chaotic oscillators,” *Phys. Rev. E* (in progress).

## Conference Proceedings and Talks (16)

16. Kozma, R., Davis, J.J.J., Freeman, W.J., “Neurophysiological evidence of the cognitive cycle and the emergence of awareness,” *Int. Conf. Awareness Sci. & Tech. iCAST2013*, Nov. 1-5, 2013, Aizu-Wakamatsu, Japan, IEEE Press (2013).

17. Erdi, P., Kozma, R., Puljic, M., Szente, J. “Neuropelation and Related Models of Criticalities.” In *Contents XXIX-th Eur. Meeting of Statisticians*, Hungary, Aug., 2013, pp. 106.

18. Kozma, R., Rosa, J., Piazzentin, D. “Cognitive Clustering Algorithm for Efficient Cybersecurity Applications,” *Proc. IEEE/INNS Int. Conf. Neur. Networks IJCNN2013*, Aug. 4-9, Dallas, TX, USA, pp. 471-478, IEEE Press, 2013.

19. Ilin, R., Kozma, R., “Detection of Spatiotemporal Phase Patterns in ECoG Using Adaptive Mixture Models,” *Int. Joint Conf. Neural Networks (IJCNN2013)*, Dallas, TX, August 3-7, 2013.

20. Kozma, R. “The race to new mathematics of brains and computers – Tribute to John G. Taylor,” *Proc. IEEE/INNS Int. Conf. Neur. Networks IJCNN2013*, Aug. 4-9, 2013, Dallas, TX, USA, pp. 21-23, IEEE Press, 2013.

21. Kozma, R., “Criticality and noise in brains and nuclear reactors – Similarities and differences,” *Invited Talk, Chalmers University*, Goteborg, Sweden, June 28, 2013.

22. Kozma, R., Freeman, W.J. (2013) “Modeling cortical singularities during the cognitive cycle using random graph theory,” *Proc. Int. Conf. Cognitive Neurodynamics*, Sigtuna, Sweden, June 20-25, 2013, Springer Verlag (in press, 2013).

23. Freeman, W.J., Kozma, R., Li, G., Quiroga, Q.R., Vitiello, G., Zhang, T. (2013) “Advanced models of cortical processing in perception.” *Proc. Int. Conf. Cognitive Neurodynamics*, Sigtuna, Sweden, June 20-25, 2013, Springer Verlag (in press, 2013).

24. Kozma, R. (2013) “Metastable activity patterns in cortical dynamics and the illusion of localized representations.” *Proc. Int. Conf. Cognitive Neurodynamics*, Sigtuna, Sweden, June 20-25, 2013, Springer Verlag (in press, 2013).

25. R. Kozma, J. Rosa, D. Plazentin “Analyzing Social Networking Data using a Neuromorphic Algorithm,” Presented at *CyberSci Summit*, June 25-26, 2013, Arlington, VA.

26. Davis, J.J., R. Kozma “Creation of Knowledge & Meaning Manifested via Cortical Singularities in Cognition,” IEEE Symp. Ser. Comp. Intell. SSCI2013, April 13-17, 2013, Singapore (2013).

27. Kozma, R., J.J.J. Davis “On the Invariance of Cortical Synchronization Measures Across a Broad Range of Frequencies,” *Inf. Conf. Awareness Sci. & Technology iCAST2012*, Seoul, Korea, pp. 280-285, 2012.

28. Kozma, R., Puljic, M. (2012) “Learning Effects in Coupled Arrays of Cellular Neural Oscillators,” *Int. Conf. Brain Inspired Cognitive Systems BICS2012*, July 11-14, 2012, Shenyang, China.

29. Freeman, W.J., Kozma, R., G. Vitiello (2012) "Adaptation of the Generalized Carnot Cycle to Describe Thermodynamics of Cerebral Cortex," *Proc. IEEE World Congress Comp. Intellig. WCCI/IJCNN 2012*, Brisbane, Australia, June 10-15, 2012, IEEE Press, pp. 3229-3236.
30. Davis, JJ. Joshua, Kozma, R. (2012) "Analysis of Phase Relationship in ECoG using Hilbert Transform and Information Theoretic Measures," *Proc. IEEE World Congress Comp. Intellig. WCCI/IJCNN2012*, Brisbane, Australia, June 10-15, 2012, IEEE Press, pp. 887-893.
31. Freeman, W.J., Kozma, R., Vitiello, G (2012) "Adaptation of the Generalized Carnot Cycle to Describe Thermodynamics of Cerebral Cortex," *Proc. IEEE World Congress Comp. Intellig. WCCI/IJCNN12*, June, 2012, Brisbane.

#### 4. Meetings and additional deliverables (9)

- Attending PI Re-launch meeting at HRL, Malibu, CA, October 9-10, 2012.
- Attending experiment-theory implementation lab visits at UCLA, Gimzewski/CASA team and UCB/WJFreeman, November 28- December 1, 2012.
- Participating at DARPA teleconferencing with DARPA managers and PI team members, December 6, 2012.
- Special Session organized at Int. Conf. on Cognitive Neurodynamics: "Advanced Models of Cortical Dynamics in Perception," W.J. Freeman (organizer), R. Kozma, R. Quiroga, G. Vitiello (invited speakers), Sigtuna, Sweden, June 23-27, 2013.
- Project meeting on January 30, 2013 at UCB with the participation of U of Memphis (R. Kozma) with PI team members from UCB (W.J. Freeman), and UCLA (J. Gimzewski, A. Stieg, H. Sillin).
- Preparation of PI project Memephis April 11-12, 2013, in Memphis with representatives of all contributing teams.
- April 11-12, 2013: Physical Intelligence Team Meeting hosted by R. Kozma, at the University of Memphis. 8 team members from HRL, UCLA, SRI, and U of Memphis attended the 2-day meeting in preparation for the upcoming program review at HRL. <http://clion.memphis.edu/events/darpa-pi-2013/>.
- April 29-30: Attending Physical Intelligence Program Review Meeting at HRL and presenting results by the neuropercolation team.
- Attending DARPA teleconferencing for the Physical Intelligence Program, Phase II, Program Review, July 16, 2013.